EFFECT OF NYLON-6 AND CHITOSAN NANOFIBERS ON THE PHYSICO-

MECHANICAL AND ANTIBACTERIAL PROPERTIES OF AN

EXPERIMENTAL RESIN-BASED SEALANT

by

Maria Fernanda Hamilton

Submitted to the Graduate Faculty of the School of
Dentistry in partial fulfillment of the requirements for the
Degree of Master of Science in Dentistry, Indiana
University School of Dentistry, June 2014.

Thesis accepted by the faculty of the Departments of Operative and Preventive Dentistry, Indiana University School of Dentistry, in partial fulfillment of the requirements for the degree of Master of Science in Dentistry.

Richard L. Gregory

Armando Soto

Andrea Ferreira Zandona

Marco C. Bottino
Chair of the Research Committee

Norman B. Cook
Operative Program Director

Anderson Hara
Preventive Program Director

Date

ACKNOWLEDGMENTS

inspiration. To my husband, Tim, thank you for everything you do for me, for all the support over the past few years. I love you so much more than words can express.

Last, but not least, I would like to thank my friends and my Operative Graduate Program family for all the laughs, support, and motivation during my stay at IUSD.

TABLE OF CONTENTS

LIST OF ILLUSTRATIONS

INTRODUCTION

The increased recognition of the causes of dental caries, and a better understanding of the disease process have led practitioners to prefer a preventive and minimally invasive approach to treatment.[1]

A successful treatment to arrest the progression of incipient pit and fissure carious lesions are "pit and fissure sealants." The term is used to describe a type of material that, when applied to pits and fissures of susceptible teeth, forms a protective layer preventing the invasion of bacteria and plaque accumulation. Furthermore, it hinders the access of the bacteria's source of nutrients.[2]

Pit and fissure sealants were commercially introduced in 1971 with the early studies of Buonocore.[1] Since then, numerous investigations have shown effectiveness in the reduction and progression of caries in children and adolescents.[3-7]

The effectiveness of a fissure sealant depends of its retention. Similar to resin composite restorations, resin-based dental sealants also undergo degradation in the oral environment, often leading to failure of the material[8] and therefore reduction of its protective role.

Electrospinning is a technique that uses electric forces to fabricate ultrafine fibers with complex, three-dimensional (3D) architecture of various polymers. In this process, fiber diameter ranges typically from a few nanometers to a few microns.[9,10]

Chitosan is the deacetylated form of chitin.[11] This nontoxic biopolymer has received significant attention due to its biocompatibility, antioxidant, anti-inflammatory and antibacterial properties.[12] These bioactive properties make chitosan an ideal natural

polymer for application in different fields such as medicine, dentistry,[12-14] food and agriculture industries.[15,16] Meanwhile, nylon is a polyamide with important properties regarding strength, flexibility, and resistance to abrasion.[17] Owing to these properties, nylon has been used in different industries such food, automobile, electronics, as well as in medicine in the production of suture materials.[17,18]

Relevant to the scope of the present study, the literature has reported that the addition of a wide variety of fillers (e.g. boro-silicate glass, nylon-6, rayon, E-glass, polyethylene and others) to resin-based materials improves hardness, compressive strength, stiffness, impact resistance, and decrease water sorption.[19-21] Therefore, the objectives of this *in-vitro* study were to develop experimental resin-based sealants containing chitosan and nylon-6 nanofibers obtained via electrospinning and to evaluate their chemical, physico-mechanical and antibacterial properties.

HYPOTHESIS

The null hypothesis to be tested was that there would not be a significant difference in the effect of the physico-mechanical and antibacterial properties of the experimental sealants when compared with Helioseal Clear, a commercially available sealant.

REVIEW OF LITERATURE

PIT AND FISSURE SEALANTS – A BRIEF OVERVIEW

Dental sealants applied to the enamel tooth structure form a barrier that isolates pit and fissures from saliva, food. and dental plaque.[22]

The first report in the literature of sealing fissures was in 1895, when Wilson published a technique using oxyphosphate cement to seal fissures.[23] Later, the revolutionary acid-etch technique proposed by Buonocore [24] in 1955 yielded, in the late 1960s, the first clinical trial of pit and fissure sealants by Cueto and Buonocore.[25] Evidence eventually showed that use of sealants can arrest caries progression of non-cavitated lesions in permanent teeth in children, adolescents, and young adults, and these findings led the Centers for Disease Control and Prevention (CDC) and the American Dental Association (ADA) to recommend the use of sealants as a component of oral care.[26-28]

The main materials used as sealants are 1) resin-based sealants, available as autopolymerized or photopolymerized, and 2) glass-ionomer cements, available as conventional and resin-modified glass ionomer.[28,29] Unfortunately, glass-ionomers sealants have shown a lower retention rate and greater microleakage when compared with resin-based sealants.[30,31]

Considering that dental sealants form a physical barrier to prevent pit and fissure caries, the retention rate becomes a main factor for its effectiveness[32]. Soto-Rojas et al.[22] reported a retention rate of resin-base sealant after 1 year, 2 years, and 4 years of 96.4

percent, 86.7 percent, and 60.6 percent, respectively, indicating that the survival of the

sealant decreased as the age of the sealant in the mouth increased.

Further, sealants may not perfectly bond to enamel, creating a gap in the sealant-

enamel interface that might allow the adhesion and penetration of microorganisms,

resulting in failure of the sealant.[33,34] Therefore, research has focus in the incorporation of

filler materials into fissure sealants that might provide antibacterial, remineralization or

mechanical enhancement benefits. The introduction of fillers in resin-based materials

plays a role in their mechanical behavior.[35] Filler-reinforced dental composites have

demonstrated increased wear resistance, flexural strength, elastic modulus, work of

fracture, compressive strength, stiffness, and decrease of water sorption.[35-37] Similarly,

the introduction of filler particles into fissure sealants has shown to enhance the surface

texture and wear resistance and hardness.[31,38]

Nonetheless, a wide variety of materials have been incorporated into resin-based

sealants aiming to achieve remineralizing and/or antibacterial properties:

Fluoride

Several studies have looked at the potential benefit of adding fluoride into resin-

based fissure sealants, as additional caries protection. Laboratory studies of resin-based

sealants containing fluoride have shown it to reduce enamel demineralization[39] and that

enamel hardness decreased the values[40] of caries-like lesions. On the other hand,

conflicting results were reported by Vatanatham et al.[41] where no significant difference

was found in the mineral loss of incipient enamel carious lesion sealed with fluoride-

containing and nonfluoride-containing sealants. The discrepancy of these findings might

be explained by the use of different materials and methodology.

Fluoride-containing resin-based sealants have also shown growth inhibition

properties against *L. acidophilus* and *S. mutans*.[42] Ideally, a fluoride containing material

should be able to release an active level of fluoride for a prolonged period of time to be

effective.[43] Fluoride-containing sealants have shown to have a "burst effect," where great

amounts of fluoride are released during the first days, and then the release diminished

over time.[44,45]

Simonsen in his literature review[46] pointed out that the incorporation of fluoride

to resin sealants is more a marketing strategy than a clinical benefit, because few studies

show a clinical advantage. Also, poor retention rates of fluoride-containing resins in

comparison with nonfluoride-containing sealants have been reported.[47]

Amorphous Calcium Phosphate (ACP)

Resin-based sealants containing ACP have been able to remineralized enamel

carious lesions *in situ*.[48]

Methacryloxylethyl Cetyl Demthyl
Ammonium Chloride (DMAE-CB)

The incorporation of DMAE-CB into a commercial fissure sealant at 1 wt% has

shown to provide antibacterial activity without compromising the properties of the

material.[49]

Surface Reaction-Type Pre-Reacted Glass-Ionomer (S-PRG)

Fissure sealants containing S-PRG have demonstrated inhibition of demineralization, enhancement of remineralization, and superior fluoride release and recharge than commercial sealants that contain fluoride.[50]

ELECTROSPINNING

Nanotechnology is an area of science that has gained increased attention in the past two decades. One principle of nanotechnology is the reduction of materials to ultra-thin dimensions leading to new and improved properties.[51] For instance, nanofibers present excellent structural mechanical properties, flexibility combined with high axial strength; high aspect ratio, i.e., length/diameter (l/d); and high surface area.[52]

Polymeric nanofibers are generally produced from synthetic, natural, or a blend of polymers. There are several methods to fabricate nanofibers, including melt-blown and electrospinning.[51] Melt-blown has shown significantly higher productivity than electrospinning. However, electrospinning allows more controlled fiber diameters and allows processing polymers and additives of all kinds.[51]

The basic process of electrospinning takes place in a polymer solution pumped through a nozzle. Additionally, the nozzle serves as an electrode to which a high electric field is applied using a DC voltage.[51] When this high voltage is applied reaching a threshold that overcomes the surface tension of the polymer solution, it causes a cone-shape deformation (i.e., Taylor Cone) of the solution. The solution leaves the cone as a jet, and the solvent evaporates, leading to the formation of fibers that are collected into a substrate, usually an aluminum foil sheet, brought into contact with a grounded metallic

plate (counter electrode). The continuous deposition of the fibers leads to the formation

of non-woven mats, the arrangement of which is defined by the counter electrode.[51,53,54]

During electrospinning it is important to considerer certain parameters that can

influence the dimensions and structures of the nanofibers. These parameters include: the

polymer solution (viscosity, solubility, temperature, elasticity, conductivity, etc.); process

parameters such feed rate, electric potential at the capillary tip, distance between the tip

and the collector, applied voltage, and environmental parameters such humidity and air

velocity in the electrospinning chamber. The choice of parameters provides a range of

possibilities for the target electrospun materials.[9,10] Figure 1 shows a schematic

representation of the setup for the electrospinning process.

CHITOSAN

Chitin, is a natural mucopolysaccharide found in shells of crustaceans, insects,

and fungi. After cellulose, it is the most abundant organic material.[55]

Chitosan, (1–4)-linked 2-amino-2-deoxy-D-glucopyranose is a biocompatible,

nontoxic biopolymer product of deacetylation of chitin. In recent years chitosan and its

oligosaccharides have received significant attention in various industries due to their

antioxidant, anti-inflammatory, antimicrobial, immuno-stimulating and anticancer effects,

as well, as a drug delivering system.[56] Owing to these properties, chitosan has been

investigated in different areas of dentistry, including endodontics,[57] oral surgery,[58]

periodontics,[59] and preventive and restorative dentistry.[60]

Chitosan differs greatly in its molecular weight (MW) and degree of deacetylation (DA). It depends on the source of chitin and the methods of hydrolysis. The MW can vary from 30 kDa to > 1000 kDa, and typically its DA is greater than 70 percent.[61]

The antimicrobial properties of chitosan have shown activity against a variety of microorganisms, including bacteria[62] and fungi.[63] The mechanism of action for its antimicrobial properties is still unknown; however, three different mechanisms have been proposed.[64] First, due to its cationic charge, chitosan reacts with the anionic surfaces of the microorganism; damaging the cell membrane.[65] Second, chitosan acts as a chelating agent and binds to trace elements necessary for normal growth of microorganisms.[66] Third, it has been proposed that chitosan binds with DNA, inhibiting the synthesis of mRNA and proteins.[64,67]

The antimicrobial activity of chitosan differs with the type of chitosan (intrinsic factors) and extrinsic factors; mainly molecular weight, degree of deacetylation, target organism and the conditions of the medium in which it is applied (pH, ionic strength, and the presence of solutes susceptible to react with chitosan blocking the reactivity of the active amine groups).[68]

Streptococcus mutans grows on the enamel in biofilms and is considered the main etiological agent of dental caries.[69,70] An *in-vitro* study on the effect of chitosan on *S. mutans* has shown that low-molecular weight chitosan and its derivatives are able to inhibit sucrose-dependent and independent attachment of *S. mutans* to saliva-coated or uncoated hydroxyapatite.[71] Furthermore, it has been shown that chitosan reduces *S. mutans* viability on biofilms; and chitosan nanoparticles have the ability to impede acid tolerance response induction in adhered *S. mutans*.[72,73]

Mahapoka et al.[60] showed that the addition of chitosan whiskers into experimental resin-based sealants presented antimicrobial activity against *S. mutans* (UA 159), when compared with an experimental resin-based sealants without chitosan whiskers and a conventional available sealant (Delton, Dentsply, IL). Furthermore, this property was comparable with existing commercial resin sealants that claim to present antimicrobial properties, such as: the fluoride-containing resin sealant (Teethmate F-1, Kuraray Medical, Kusashiki, Japan); and a triclosan-containing dentin sealant (Seal&Protect, Dentsply). Moreover, the addition of chitosan whiskers did not reduce the curing depth, degree of conversion, or hardness of the experimental sealants.[60]

NYLON-6

Nylon-6 (poly-(ε-caproamide) or polyamide) was discovered in 1938 by Schlack with its first production in Germany in 1940. During World War II, nylons were mainly used for military purposes; however, after the war, nylons were produced by many countries on an increasing scale for civilian applications (e.g. textile fabrics, membranes, electronics, food packing, automotive parts, etc.).[17,74]

Approximately 80 percent of its use is in synthetic fibers, and the remaining 20 percent, in engineered resins. As engineered resins, nylons show high thermal stability, high resistance to impact and abrasion, and good resistance to organic solvents.[74]

Processing parameters for optimal fabrication of nylon-6 nanofibers via electrospinning have been investigated. Overall, nylon-6 nanofibers have shown good mechanical properties, such high tensile strength and fracture toughness.[75,76] During electrospinning the jet is elongated up to 100,000 times in less than one tenth of a

second[77]; resulting in an extremely large draw ratio, which can closely align macromolecular chains along the fiber axis, making the electrospun fibers mechanically strong. As well, the small diameter of nanofibers provides a large ratio of surface area to volume. Finally, electrospun nanofibers are continuous, they can reinforce matrixes by impeding crack propagation, if the long axis is aligned against the applied force.[78]

Therefore, electrospun nylon-6 nanofibers have been used successfully to reinforce resins such as polyaniline, melamine-formaldehyde, poly (methyl methacrylate), and bis-glycidyl methacrylate/tetraglycidylmethacrylate (BIS-GMA/TEGDMA) as dental restorative composites.[36,79-81] For example, Fong and colleagues[36] found that the layer-by-layer incorporation of nylon-6 nanofiber sheets into a resin composite led to an effective reinforcement of dental composites. The incorporation of small amounts (5-percent mass fraction) into a BISGMA/TEGDMA mixture, improved the flexural strength by 36 percent, elastic modulus by 20 percent, and work of fracture by 42 percent of the experimental resin.

RATIONALE OF THE STUDY

The purpose of this *in-vitro* study was to develop and evaluate experimental resin-based sealants containing electrospun nylon-6 and chitosan nanofibers in an attempt to improve the mechanical properties and provide an antibacterial protective effect, respectively.

MATERIALS AND METHODS

This *in-vitro* study evaluated the chemical, physico-mechanical and antibacterial properties of experimental resin-based sealants containing electrospun nanofibers (i.e., pure chitosan, and pure Nylon-6) and a commercially available sealant.

PREPARATION OF ELECTROSPUN NANOFIBERS

Solution Preparation

Practical-grade chitosan (Sigma – Aldrich Corp., St. Louis, MO), molecular weight ~190,000-375,000 Da, and ≥ 75-percent deacetylated was dissolved in Trifluoroacetic acid (TFA) (Sigma – Aldrich Corp.) and Dichloromethane (DCM) (Acros Organics, NJ) (60:40 TFA/DCM) to obtain a 7 wt% chitosan solution.

Nylon-6 (Sigma – Aldrich Corp.) was dissolved in 1,1,1,3,3,3-hexafluoro-2-propanol (HFP) (Sigma – Aldrich Corp.) to obtain a 10 wt% nylon-6 solution.

The solutions were homogenized by means of magnetic stirring for at least 72 h for chitosan and 24 h for nylon-6 at room temperature.

Electrospinning Procedure

The electrospinning methodology for nanofibers processing was selected from previous published protocols for the distinct polymers,[36,82] and optimized as needed in order to obtain defect-free chitosan and nylon-6 fibers.

Five milliliters of each polymer solution was placed into a plastic syringe capped with a 27-gauge metallic needle (Small Parts, Inc., Miami, FL). The syringe then was

placed on an automatic syringe pump (KDS 200 Legato - Holliston, MA), which was at a fixed distance from the negative electrode. The positive electrode of a high-voltage power supply (Gamma Voltage Research Inc., Ormond Beach, FL) was connected to the needle by means of an alligator clip. The electrospun nanofibers were collected over an aluminum foil wrapped grounded rotating stainless steel mandrel in the case of nylon-6 and chitosan was collected over an aluminum foil sheet on a static plastic plate, at different distances from the needle tip, 18 cm and 15 cm respectively. Chitosan nanofiber fabrication was achieved by applying 25 kV voltage to the polymer solution, delivered at a constant flow rate of 1.0 mL/h. For nylon-6, a voltage of 10 to 18 kV was applied, delivered at a constant flow rate of 1.0 mL/h. The electrospun mats were kept in a vacuum desiccator for 48 h at room temperature to remove any residual solvent.

CHARACTERIZATION OF NANOFIBERS

Morphological Characterization

For the morphological characterization of electrospun fiber mats, small samples (n = 4) were cut and mounted in an aluminum stub and sputter-coated with a thin layer of gold to allow better electrical conduction.

The average fiber diameter was determined from scanning electron microscope (SEM) (JSM-6390, JEOL, Tokyo, Japan) (Figure 2) images by measuring the diameter of 120 fibers from three different images for nylon-6, and seveb different images for chitosan at the same magnification using Image-Pro Plus software (Media Cybernetics Co., Bethesda, MD).

Chemical Characterization

Fourier transform infrared (FTIR) (Thermo Fisher Co, Waltham, MA) spectroscopy (Figure 3) was used in attenuated total reflection mode to distinguish the chemical structure and phase composition of the different nanofibers in the wavelength range of 4000-800 cm^{-1}.

EXPERIMENTAL RESIN-BASED SEALANT

Formulation of the Experimental Resin-Based Sealant

The formulation for the experimental sealant followed one described elsewhere.[83] It consisted of a 60 percent by weight of bisphenol A Bis (2-Hydroxy-3-Methacryloxypropyl) ether (Bis-GMA) and 40 percent by weight of triethyleneglycol dimethacrylate (TEGDMA) (ESSTECH Inc., Essington, PA) mixture. Camphorquinone (CQ) (ESSTECH Inc.) at 0.5 percent by weight, as a photoinitiator, and 2-(Dimethylamino)ethyl methacrylate (DMAEMA) (Sigma – Aldrich Corp.) at 1 percent by weight, as co-initiator were added to the resin.

Electrospun Fibers Filler Preparation

For the incorporation of nanofibers into the experimental sealants, a modification of a published protocol by Tian et. al.[78] was followed. In brief, cut pieces of chitosan and nylon-6 electrospun mats ($\sim 3 \times 3$ cm^2) (Figure 4) were immersed into the aforementioned resin mixture. Upon complete visual impregnation, the soaked mat pieces were carefully removed and placed on a glass plate. A Mylar sheet and a glass plate were placed on top of the samples and with light pressure the excess of material and air bubbles were removed (Figure 5). The samples were then transferred into a TRIAD 2000

chamber (DENTSPLY International, Inc. York, PA) (Figure 6) for photopolimerization

for 2 min. The final composites had a nanofiber content of 20 wt% (Figure 7).

CRYOMILLING PROCEDURE

      To allow the introduction of the fabricated nanofibers within the experimental

resin-based sealant, the composites plates containing nanofibers, underwent a cryomilling

(Spex CertiPrep 6750 cryogenic impact mill - Metuchen, NJ) (Figure 8) process to obtain

a fine micron-sized powder. Samples of composites plates containing the nanofibers,

were milled for 15 min and precooled for 2 min before the milling process.

The milling consisted on alternating cycles of 1 min, separated by cooling intervals of 1

min. Liquid nitrogen surrounding the milling machinery was used to ensure complete

cooling during cycles. Images of cryomilling samples (powder) were obtain using SEM

(JSM-6390, JEOL) to determine morphology and particle-size distribution of the milled

samples. Additionally, the particle-size distribution of the cryomilled samples was

measured by a laser granulometer (Cilas 1064; Cilas, Marseille, France).

INCORPORATION OF THE NANOFIBERS INTO RESIN SEALANTS

      The formulation for the experimental sealants followed the same formulation as

described above. The monomers were mixed by hand spatulation and then homogenized

by means of magnetic stirring for 24 h in a constant temperature room (20°C). After 24 h,

the initiator and co-initiator were added in similar manner. The resin-based sealants were

prepared at three different filler levels by weight percent. Cryomilled samples of N6 and

CH were mixed with the experimental resin-based sealant, as previously described, to

obtain groups containing 1 percent, 2.5 percent, and 5 percent by weight of Nylon-6 and groups containing 1 percent, 2.5 percent, and 5 percent by weight of CH.

To ensure complete homogenization after incorporation of the fillers into the experimental sealants, the mixtures were left overnight on magnetic stir plates. Then, the mixtures were kept under vacuum overnight to eliminate trapped air bubbles that might have occurred during the homogenization.

Experimental sealant without nanofibers and an unfilled commercial light-curing fissure sealant (Helioseal Clear, Ivoclar-Vivadent, Amherst, NY) (Figure 9) served as negative control and commercial reference, respectively.

Table I shows the chemical composition of the commercially available light-cured sealant Helioseal Clear and of the experimental groups.

PHYSICO-MECHANICAL PROPERTIES

Flexural Strength (FS)

For the flexural strength (FS) test,[83] 11 samples of each group were prepared using a stainless steel split mold (2 mm in depth by 2 mm in width by 25 mm in length). The specimens were light-cured for 40 s placing the light tip in different positions to assure complete exposure (Figure 10).

To assure consistency between groups, the curing light (DEMI, Kerr Corporation, Middleton, WI) was monitored periodically by means of a radiometer (Cure Rite, Dentsply Caulk, Milford, DE) with an average power density output of $>700 \text{mW/cm}^2$.

To remove flash and irregularities, the periphery of the samples were wet-finished with 320-grit and 600-grit abrasive papers. Prior to testing, the specimens were stored at 37^0C for 24 h.

The FS was conducted using a three-point bending jig adapted in a universal testing machine (Instron ElectroPuls 3000, Norwood, MA). The span between the supports was set at 20 mm and the cross-head speed at 1 mm/min. Figure 11 shows FS testing procedure.

The load and the corresponding deflection were recorded and calculated using Bluehill 2 software (Instron) in which the following formula was applied:

$FS = 3Pl/2bd^2$

Whereas:

p = load at fracture (N)

l = distance between supports (20 mm)

b = width of the specimen (mm)

d = depth of the specimen (mm)

Vickers Microhardness

For the Vickers microhardness test,[83] nine samples per group were prepared using a round mold (2 mm in height by 5 mm diameter). The samples were prepared, light-cured and stored as previously described for FS test (Figure 12).

To finished and polished the samples water-cooled abrasive discs (1200, 2400, and 4000-grit SiC papers) (MD-Fuga, Struers Inc, Cleveland, OH) and polishing cloth (MD-Nap, Struers Inc.) with diamond suspension (1 µm, Struers Inc.) were used. After

polishing, the samples were submerged in deionized water for 3 min and later sonicated

in detergent solution for 3 min (for complete removal of the diamond suspension), and

then again submerged in running deionized water for 3 min. A load of 100 g was applied

on the surface of the samples by means of a diamond indenter attached to a

microhardness tester (LECO LM247AT, LECO Corp., St. Joseph, MI). Five

measurements were obtained from each sample and averaged. Figure 13 shows a

representation of the Vickers microhardness test procedure. The Vickers hardness

number (VHN) was calculated by measuring the length of the diagonal of the indentation.

The measurements were recorded and calculated using Leco ConfiDent 2 software

(LECO Corporation) in which the following formula was used:

VHN= 1854.4 x P / d^2

Whereas:

 P = load (g)

d = mean diagonal of the indentation (μm)

ANTIBACTERIAL ASSAY

Agar Diffusion Test

        Ten samples of each experimental group were prepared, cured and stored as

previously described for the Vickers microhardness test.

        To remove flashes and irregularities, the top and bottom of the samples were

finished with four alternating upward and downward vertical movements with 600-grit

and 1200-grit SiC papers and water cooling.

Then, the samples were sonicated (2X) in deionized water for 6 minutes. The samples were disinfected with 70-percent ethanol solution for 30 min, before testing.

For the agar diffusion test, a modification of a published antibacterial assay was followed.[60] The microorganism used for this study was *S. mutans* (UA159). Tryptic Soy broth (TSB) (Becton, Dickinson and Company, Sparks, MD) culture (5 mL) of *S. mutans* in mid-log phase (approximately 16 h) was grown and used for the inoculum.

After disinfection, the samples were placed on blood agar plates (bioMerleux, Inc. Durham, NC) containing a freshly swabbed *S. mutans* (UA159) lawn of bacteria and later incubated at 37°C for 24 h under 5-percent CO_2. The radius of the bacterial inhibition zones of each group were measured in millimeters at 24 h, 48 h and 120 h, rotating the plates each time. The tests were performed in triplicate.

Specimens without nanofibers and the commercial sealant, Helioseal Clear (Ivoclar-Vivadent) were used as negative control groups. Chlorhexidine (CHX) at 0.12-percent solution was used as a positive control group.

STATISTICAL METHODS

All data were processed by the SAS software package, version 9.3 (SAS Institute Inc., Cary, NC). The effect of study group on flexural strength, microhardness, and fiber diameter was analyzed using one-way ANOVA. Because of non-homogeneous group variances, an overall variance estimate across groups was not used in the ANOVA. Pair-wise comparisons between groups were made using Fisher's Protected Least Significant Differences to control the overall significance level at 5 percent.

SAMPLE SIZE JUSTIFICATION

Estimates of the within-group standard deviations were taken from previous studies: 12 for flexural strength[84]; and 0.5 for VHN; and 0.2 for diameter of inhibition zone.[60] All calculations assume 80-percent power for two-sided tests conducted at a 5-percent significance level.

With 11 specimens per group the study was able to detect differences of 15 MPa for flexural strength between groups. With 10 specimens per group the study was able to detect differences of 0.27 for diameter of inhibition zone. With nine specimens per group the study was able to detect differences of 0.75 for VHN.

RESULTS

MORPHOLOGICAL CHARACTERIZATION OF NANOFIBERS

Representative SEM micrographs at different magnifications of the electrospun nylon-6 and chitosan mats are shown in Figures 14 and 15, respectively. As seen in the SEM micrographs, nylon-6 exhibited a bead-free, interconnected network of randomly oriented fibers. Chitosan, on the other hand, presented randomly oriented fibers with the presence of fiber branching. Means, respective standard deviations ($\pm$ SD), standard errors ($\pm$ SE) and ranges of the fiber size diameter are presented in table II. The mean fiber diameter, for nylon-6 and chitosan was calculated by averaging the diameter of 120 fibers. The average fiber diameter for nylon-6 was found to be 503$\pm$304 nm and 595$\pm$411 nm for chitosan. There was not a significant difference between nylon-6 and chitosan fiber diameter ($p = 0.0601$).

CHEMICAL CHARACTERIZATION OF NANOFIBERS

IR spectra was taken in the spectral range of 4000 – 800 cm^{-1} of bulk practical grade (PG) chitosan powder, as well as electrospun nylon-6 and chitosan mats. Figure 16 displays IR spectra of nylon-6 electrospun mat (top), chitosan electrospun mat (middle) and bulk PG chitosan (bottom) in a narrower spectral range (2000-800 cm^{-1}).

Analysis for PG chitosan (bulk) and electrospun chitosan indicated characteristic peaks associated to N-H stretching including NH_3^+ (1650 cm^{-1} and 1576 cm^{-1}) and C-O stretching and saccharide groups (893 cm^{-1}, 1065 cm^{-1}, 1150 cm^{-1}, 1198 cm^{-1}) for PG chitosan and 896 cm^{-1}, 1067 cm^{-1}, 1137 cm^{-1}, 1192 cm^{-1} for electrospun chitosan.

Peaks at 1671 cm^{-1} and 839 cm^{-1} were observed for electrospun chitosan, indicating presence of remaining solvent (TFA).

FTIR analysis for nylon-6 indicated its characteristic molecular structure that consist of amide groups (CO-NH) and methylene segments [-(CH$_2$)$_5$-]. The characteristic absorption bands were observed at 3290 cm^{-1} (hydrogen-bonded NH stretching), 3085 cm^{-1} (NH Femi resonance) 2932 cm^{-1} (CH$_2$ asymmetric stretching), 2859 cm^{-1} (CH$_2$ symmetric stretching), 1637 cm^{-1} (amide I), 1544 cm^{-1} (amide II), 1369 cm^{-1} (amide III + CH$_2$ wagging), 1261 cm^{-1} (amide III + CH$_2$ wagging), 1171 cm^{-1} (CONH skeletal motion), 973 cm^{-1} (CONH in-plane ($_\gamma$)).

EXPERIMENTAL RESIN-BASED SEALANT CRYOMILLING PROCEDURE

As previously described, to allow the introduction of the fabricated nanofibers within the experimental resin-based sealant, the composites plates containing the nanofibers underwent a systematic (cryomilling time was used as a variable) cryomilling process. Representative SEM micrographs of the nylon-6 milled particles are shown in Figures 17(A-B). Figure 18 exhibits the presence of randomly distributed nylon-6 fibers. SEM images of the chitosan milled particles are shown in Figures 19(A-B).

The particles present an irregular shape with an average size distribution of 15.87 μm for nylon-6 and 14.24 μm for chitosan. Representative SEM micrographs of the milled particles from a pilot study (1 minute and 8 minute cryomilling) are shown in Figures 20 to 23. Nylon-6 milled at 1 min presented an average particle size distribution of 81.30 μm and 33.24 μm at 8 min. For chitosan the average size distribution at 1 min was 112.97 μm and 26.03 μm at 8 min. Evidence of intact nylon-6 and chitosan

nanofibers are presented in Figures 20(A-C), 21(B) and 23(B) at these different

cryomilling times.

PHYSICO-MECHANICAL PROPERTIES OF
THE EXPERIMENTAL SEALANTS

Flexural Strength (FS)

Means, respective standard deviations (± SD), standard errors (± SE) and ranges

for FS are presented in table III and Figure 24. Chitosan (5 percent) group had

significantly higher flexural strength (115.3±4.5 MPa) than all other groups (p = 0.0000).

Chitosan (1 percent) at 110.1±3.5 MPa and chitosan (2.5 percent) at 109.3±3.4 MPa

groups had significantly higher flexural strength than the control (unfilled) (p = 0.0016

and p = 0.0033 respectively), Helioseal Clear (p = 0.0000), and nylon groups. Nylon (5

percent) at 105.0±3.3 MPa had significantly higher flexural strength than Helioseal Clear

(p = 0.0013) and nylon (2.5%) (p = 0.0250).

Figures 25 to 32 show SEM images of the different groups after FS testing. The

fractured surfaces reveal local agglomeration of randomly oriented nylon-6 nanofibers

(Figures 25(C), 26(B), and 27(B)). Higher magnification indicates the presence of broken

nanofibers, as well areas where fibers might have peeled-off from the matrix (Figures

26(B-C) and 27(C)).

Chitosan nanofibers were not able to be identified on the cryomilled samples at 15

min or on the facture surfaces (Figures 28(B), 29(B), 30(B)). However, their presence can

be confirmed on the cryomilled powder in Figure 23(B).

Vickers Microhardness

Means, respective standard deviations (± SD), standard errors (± SE) and ranges for VHN are presented in table IV and Figure 33. Chitosan (1 percent) at 38.3±0.9 had significantly higher values than all other groups, and chitosan (5 percent) at 37.0±0.3 had significantly higher values than nylon (2.5 percent) ($p = 0.0414$).

ANTIBACTERIAL ASSAY

Agar Diffusion Test

Chlorhexidine 0.12-percent solution was the only group that showed inhibition zone (4 mm) against *S. mutans* during the time of the study (24 h, 48 h and 120 h). No inhibition zone was observed in any of the other groups tested (data no shown).

Given chitosan was being tested, due to its antimicrobial properties, an agar diffusion pilot study using the chitosan and nylon-6 mats was performed.

For the pilot study, round disks of chitosan and nylon-6 mats (5 mm in diameter) were cut. Solution containing: 10 µL of chitosan disc dissolved in dimethyl sulfoxide (DMSO) (Sigma – Aldrich Corp.), 10 µL of chitosan disc dissolved in water and a pure chitosan disc were placed on blood agar plates (bioMerleux, Inc.) containing a freshly swabbed *S. mutans* (UA159) lawn of bacteria and later incubated at 37°C for 24 h under 5% CO_2. The radius of the bacterial inhibition zones of each group were measured in millimeters at 24 h, 48 h, and 120 h. The same procedure was performed for nylon-6 mats.

Upon exposure of the electrospun chitosan mat to DMSO, the fibers dissolved instantaneously. No traces of the chitosan mat seemed to remain in the solution.

Similarly, after immersion in either water or on the agar, chitosan nanofibers demonstrated a similar behavior.

The formation of halos or inhibition zones was not seen in any of the tested groups. However, what seemed to be inhibition by contact was achieved with the pure chitosan mat. The area where the chitosan mat was placed (5 mm in diameter) showed a clear area over the period of the study (up to 120 h). No other groups (chitosan in the solutions or nylon-6 groups) showed inhibition against *S. mutans* (Figures 34 and 35).

TABLES AND FIGURES

TABLE I

Sealant composition by weight percent (wt%)

Sealant	Filler Content	Resin Monomer Composition	Initiation Systems and additives
Group I	1% Nylon 6	Bis-GMA/TEGDMA 60/40 %	CQ/DMAEMA 0.5/1 %
Group II	2.5% Nylon 6		
Group III	5 % Nylon 6		
Group IV	1% Chitosan	Bis-GMA/TEGDMA 60/40 %	CQ/DMAEMA 0.5/1 %
Group V	2.5% Chitosan		
Group VI	5 % Chitosan		
Group VII	Unfilled	Bis-GMA/TEGDMA 60/40 %	CQ/DMAEMA 0.5/1 wt. %
Helioseal Clear	Unfilled	Bis-GMA/TEGDMA 60/30.3 %	Catalysts and stabilizers 0.7 %

TABLE II

Means (nm) ± SD, ± SE and ranges of the fiber diameter

Group	N	Mean	SD	SE	Min	Max
Chitosan	120	595	411	38	40	1942
Nylon 6	120	503	340	31	116	2186

TABLE III

Means (MPa) ± SD, ± SE and ranges for flexural strength (in MPa)

Group	N	Mean	SD	SE	Min	Max
Control (unfilled)	11	100.5	7.5	2.3	85.8	110.2
Chitosan 1%	11	110.1	3.5	1.1	101.0	113.1
Chitosan 2.5%	11	109.3	3.4	1.0	105.0	114.8
Chitosan 5%	11	115.3	4.5	1.3	108.0	120.6
Nylon 1%	11	102.2	4.7	1.4	93.0	108.7
Nylon 2.5%	11	100.4	5.2	1.6	92.3	107.5
Nylon 5%	11	105.0	3.3	1.0	101.8	112.4
Helioseal Clear	11	99.8	3.2	1.0	95.5	103.4

TABLE IV

Means (VHN) ± SD, ± SE and ranges for Vickers microhardness test

Group	N	Mean	SD	SE	Min	Max
Control (unfilled)	9	37.0	0.9	0.3	35.8	38.0
Chitosan 1%	9	38.3	0.9	0.3	36.8	39.8
Chitosan 2.5%	9	37.2	0.7	0.2	36.4	38.6
Chitosan 5%	9	37.0	0.3	0.1	36.6	37.6
Nylon 1%	9	37.0	0.9	0.3	36.0	38.4
Nylon 2.5%	9	36.6	0.4	0.1	36.0	37.0
Nylon 5%	9	37.2	0.9	0.3	36.2	39.0
Helioseal Clear	9	36.6	0.6	0.2	35.6	37.4

FIGURE 1.   Representative schematic of major electrospinning components and set up.
For didactic purposes the grounded mandrel/collector has been divided
into two parts to depict that electrospun fibers can be collected at a
random orientation when using very low rotating speed (A) or with high
degree of alignment by using high-speed (B). Adapted from Bottino MC,
Thomas V, Schmidt G, et al. Recent advances in the development of
GTR/GBR membranes for periodontal regeneration--a materials
perspective. Dent Mater 2012;28(7):703-21.

FIGURE 2.   Macrophotograph of the scanning electron
microscope JEOL SEM (JSM-6390, JEOL, Tokyo, Japan)
used in the study.

FIGURE 3.   Fourier transform infrared (FTIR) (Thermo
Fisher Co, Waltham, MA) spectroscopy.

FIGURE 4. Macrophotograph of an electrospun (3×3 cm^2) mat.

FIGURE 5. Macrophotograph of an electrospun mat after immersion into the BIS-
GMA/TEGDMA resin mixture.

FIGURE 6. TRIAD 2000 chamber (DENTSPLY International, Inc., York, PA).

FIGURE 7. Final composites plate with a nanofiber content of 20 wt%.

FIGURE 8.   Cryomilling machine (Spex CertiPrep 6750
cryogenic impact mill, Metuchen, NJ).

FIGURE 9.   Commercially available resin-based sealant
             Helioseal Clear (Ivoclar Vivadent, Amherst, NY).

(A)

FIGURE 10. (A) Stainless steel mold used for the flexural strength test. (B) Flexural strength specimen prepared using the mold.

FIGURE 11. (A, B) Representative macrophotographs of samples
during flexural strength testing.

FIGURE 12.   Mold and sample preparation for Vickers microhardness test.

FIGURE 13.   Representative set-up of the Vickers microhardness test procedure.

FIGURE 14.   A) and B) Representative SEM micrographs of electrospun nylon-6
nanofibers (X1500). B) Higher magnification (X5000) of the selected
area.

FIGURE 15. A) Representative SEM micrographs of electrospun chitosan nanofibers
            (X1500). B) Higher magnification (X5000 and X10000) showing
            branching of the chitosan fibers.

FIGURE 16.   FTIR spectra of electrospun nylon-6 and chitosan mats and practical grade (PG) (+) indicates the presence of remaining solvent in electrospun chitosan.

FIGURE 17. A), B) Representative SEM micrographs of cryomilled samples (15 min) containing electrospun nylon-6 fibers. B) Higher magnification (X1000). arrows indicate the presence of nylon-6 fibers.

FIGURE 18. Representative SEM micrograph showing the presence of intact randomly distributed nylon-6 fibers within the composite (X4000).

FIGURE 19.   A) and B) Representative SEM micrographs of cryomilled samples (15 min) containing electrospun chitosan fibers at different magnifications.

FIGURE 20.   A) through C) Representative SEM micrographs of cryomilled
              samples (1 min) containing electrospun nylon-6 fibers at
              different magnifications. B), C) Higher magnifications.
              Arrows indicate the presence of intact nylon-6 fibers.

FIGURE 21.   A-B) Representative SEM micrographs of cryomilled samples (8 min) containing electrospun nylon-6 fibers at different magnifications. B) Higher magnification (X1000). Arrows the presence of intact nylon-6 fibers.

FIGURE 22.   A-B) Representative SEM micrographs of cryomilled samples (1 min) containing electrospun chitosan fibers at different magnifications. B) Higher magnification (X1000).

FIGURE 23.   A-B) Representative SEM micrographs of cryomilled samples (8 min) containing electrospun chitosan fibers at different magnifications. B) Higher magnification (X1000). Arrows the presence of intact chitosan fibers.

FIGURE 24.   Mean flexural strength (in MPa).
Chitosan (5%) group had significantly higher flexural strength
(115.3±4.5 MPa) than all other groups.

FIGURE 25.   A-C) Representative SEM micrographs of the fractured surface of
               sample containing nylon-6 (1%) at different magnifications. Arrows
               indicated presence of nanofibers.

FIGURE 26.   A) to C) Representative SEM micrographs of the fractured surface of sample containing nylon-6 (2.5%) at different magnifications. Arrows indicate the presence of nanofibers.

FIGURE 27.   A) through C) Representative SEM micrographs of the fractured surface of sample containing nylon-6 (5%) at different magnifications. Arrows indicated presence of nanofibers.

FIGURE 28.   A) and B) Representative SEM micrographs of the fractured surface of
sample containing chitosan (1%) at different magnifications.

FIGURE 29.   A-B) Representative SEM micrographs of the fractured surface of sample containing chitosan (2.5%) at different magnifications.

FIGURE 30.   A) and B) Representative SEM micrographs of the
                 fractured surface of sample containing chitosan (5%)
                 at different magnifications.

60
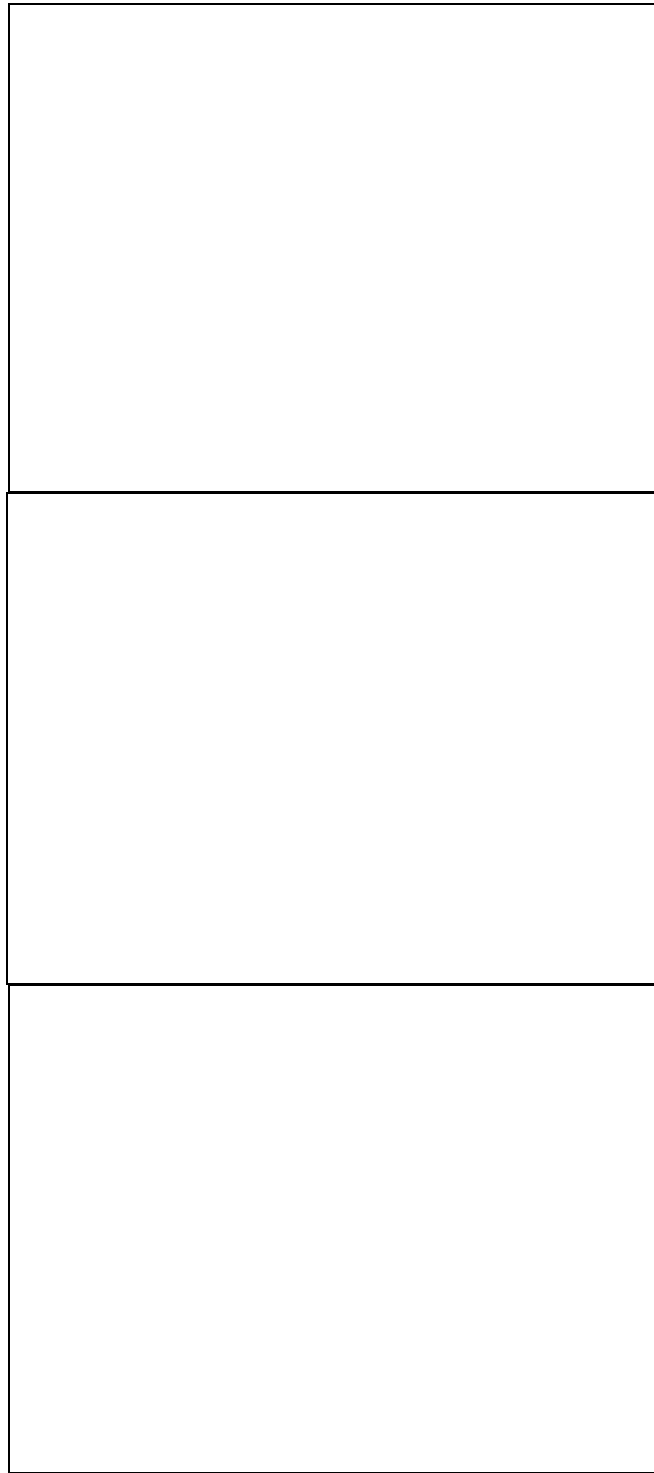
FIGURE 31. A) through C) Representative SEM micrographs of the fractured surface of
the control group at different magnifications.

FIGURE 32.   A) and B) Representative SEM micrographs of the fractured surface of
Helioseal Clear at different magnifications.

*

FIGURE 33.　　Mean Vickers microhardness number (VHN). Chitosan (1%) had
　　　　　　　significantly higher values than all other groups.

FIGURE 34.   Macrophotograph of nylon-6 agar inhibition test. No inhibition zone was seen in any of the test groups.

FIGURE 35.   Macrophotograph of chitosan agar inhibition test. A 5-mm inhibition by contact was seen on the area where chitosan mat was placed.

DISCUSSION

CHARACTERIZATION OF NANOFIBERS

Chitosan and nylon-6 nanofibers were successfully prepared via electrospinning. Fiber morphology and chemical characteristics (FTIR) are in accordance with previous studies.[11,36,61,82,85-87] As seen in Figure 14, nylon-6 electrospun mats presented beaded-free smooth randomly distributed nanofibers. This morphology was not seen on the chitosan electrospun mats, where small ramifications or "branching" were observed (Figures 15). The presence of fiber branching by chitosan may be due to alterations of the delicate balance between the electrical forces and surface tension during electrospinning This results in the decrease of the local charge per unit surface area and causes jet splitting or the formation of secondary jets.[82,88]

Schiffman et al.[11] attributed this phenomena (i.e., branching) to the presence of foreign matter that may exist on practical grade chitosan. The non-uniformity of the raw material allows branching because as the polymer solution advances, the electrostatic forces overcome the surface tension at the tip of the needle in locations where the foreign matter is possibly located.

Furthermore, Sencadas et al.[82] suggested that the mixture of the two solvents (TFA/DCM) with different boiling points may play a role in this phenomenon. The fast evaporation of DCM during the jet traveling from the needle to the collector leaves behind solidified fibers with smaller diameters than the ones that form later when the TFA solvent evaporates.

Humidity levels have also been shown to play a role in the formation of branching during the electrospinning process. Schiffman et al.[11] reported branch-free electrospun chitosan nanofibers at high humidity levels (40 percent to 45 percent). Regrettably, we did not monitor the humidity levels during electrospinning procedures. Therefore, we are not certain whether humidity has played a role in our case.

CRYOMILLED SAMPLES

As indicated in the result section, nylon-6 nanofibers were identified in the cryomilled samples and fractured surfaces. In the contrary, the identification of chitosan nanofibers in the cryomilled samples was not always possible, with the exception of the cryomilled sample at 8 min (Figure 23 (B)). The size of the fibers, in particular the branching fibers, may have made difficult their identification within the monomers.

PHYSICO-MECHANICAL PROPERTIES

The results obtained in this study were not expected since nylon-6 was introduced with the purpose of reinforcement of the experimental resin-based sealants. The overall results indicated that the chitosan groups showed significant higher FS and hardness than any other group. Chitosan fibers are considered low rigid materials which are not able to sustain force loading. However, because of its high aspect ratio, it might allow for a more efficient transfer of stresses along the fibers.[60]

The higher FS and hardness values obtained by the chitosan groups can be explained by interfacial bonding between the fibers and the matrix. Additionally, particle size and random agglomeration of the nanofibers within the sealants may have contributed to the lack of a reinforcement effect by nylon-6 nanofibers.

A coupling agent acts as a molecular bridge to form chemical bonding between the matrix and the filler. Effective coupling between the matrix and filler is necessary to achieve adequate load transfer across the filler-matrix interface; which is a condition that is needed to improve the mechanical properties of composites.[89] In fact, surface modification of fillers with coupling agents have shown to improve strength, hardness, thermal stability,[90] wear resistance,[91] fracture toughness,[92] and resistance to degradation from water[93] of resin-based materials. It is possible that the interfacial bond between chitosan and the matrix was better than the bond obtained with nylon-6. However, the nylon-6/matrix interface seemed to be somehow adequate since some of the fibers remained in close contact with the matrix and occasionally they tended to break instead of being pulled out from the matrix (Figures 26C and 27C). The surface modification of the nanofibers with a coupling agent may enhance the interfacial bonding and will be the object of study in future research to be conducted by our group. Similar observations with regard to the interface between nylon 6 nanofiber and the matrix agree with other studies.[36]

Increasing the cryomilling time could allow for obtaining finer particles. Smaller particles allow for a higher volume fraction of filler which reduces the particle interspacing as well as provides a higher total surface area for a given particle loading. Therefore, strength of the composites increases through a more efficient stress transfer mechanism.[92,94]

The agglomeration and random alignment of the nanofibers (Figures 25C, 26B and 27B) might act as flaws, weakening the composite. A better dispersion method of the filler particles would allow for a better distribution of the filler within the resin.

ANTIBACTERIAL ASSAY

The antimicrobial activity of chitosan has been investigated against a wide range of microorganisms. However, the reports of its antimicrobial activity vary, sometimes with contradictory findings. The type of chitosan (i.e., molecular weight, degree of deacetylation, etc.) and other external factors (i.e., target organism, test methodology, etc.)[68,95] may explain the unpredictability in its antimicrobial activity. Nevertheless, it is generally recognized that yeast and mold are the most susceptible groups to chitosan, followed by Gram-positive and Gram-negative bacteria.[68]

Several methods have been used to determine the antimicrobial activity of different agents, such agar dilution, broth microdilution, agar diffusion and others. The agar diffusion test is a relatively straightforward and fairly inexpensive method commonly used to examine the antimicrobial activity of various antimicrobial agents.[96]

As indicated in our results, none of the experimental resin-based sealants and controls showed halos of inhibition surrounding the discs or inhibition by contact against *S. mutans*. Chlorhexidine 0.12-percent solution was the only group that showed an inhibition zone during the time of the study (data no shown). Contradictory results were observed by Mahapoka et al.,[60] using the method of agar diffusion test, reported inhibition against (UA 159) *S. mutans* when 2 percent by weight of chitosan nano-whiskers were introduced into experimental resin-based sealants. Possible explanations in the discrepancy of our results can be due to the type of chitosan used, and the actual amount of chitosan available to interact with the bacteria.

Molecular weight (MW) and degree of deacetylation (DA) vary from the different types of chitosan; factors that influence the antimicrobial activity of chitosan

independently.[97] The DA of the chitosan whiskers in Mahapoka et al. study was similar

to the DA that is reported for practical-grade chitosan used in our study (74 percent and ≥

75 percent, respectively). The MW in their study was not reported and therefore may

have been a lower MW than practical-grade chitosan. It has been reported that lower MW

chitosans have greater antimicrobial activity than high MW chitosans. This behavior

might be explained by the easier mobility, attraction and ionic interactions of smaller

molecular chains than bigger ones, facilitating the binding with the membrane surfaces of

the target organism,[97] as well, facilitating diffusion through the agar. An effective

diffusivity through a given membrane decreases as the molecular weight of the molecule

that is being diffuse increases.[98]

Another plausible explanation in the difference in results might be related to the

actual amount of chitosan available to interact with the bacteria. In Mahapoka and

colleagues' study, pure chitosan whiskers were introduced into the resin sealant. On the

other hand, in our study the cryomilled powder that was introduced into the resin-based

sealants was a mixture of the chitosan nanofibers and polymerized monomers.

Since chitosan was used as an antibacterial agent in this study, we tested the

electrospun chitosan mat dissolved in DMSO, water, and as a pure mat to assess its

antibacterial activity. Chitosan mats were dissolved in these solutions to evaluate CH

behavior; as well to assess if the mats would provide antibacterial properties to the

solutions. DMSO was used because it will not interfere with antimicrobial activity of

chitosan; as well, it did not present an antimicrobial effect by itself at the concentrations

used in this study.

With regard to the solubility behavior of chitosan, Schiffman and colleagues[11] reported comparable solubility behavior of electrospun chitosan nanofibers when subjected to acetic acid and water. Therefore, cross-linking of electrospun chitosan fibers has been recommended as an additional step towards the development of water-insoluble materials.[11]

When the chitosan mat was directly placed on the agar, the mat disappeared instantaneously, probably due to water uptake from the agar. This behavior is consistent with a number of studies that showed chitosan's inability to diffuse through agar media and only the microorganisms with direct contact are inhibited.[99-101] The diffusion behavior depends on factors such molecule size, polarity, and shape of the material.[102]

Halos of inhibition were not observed for any of the chitosan solutions. Inhibitory activity by contact was observed only for the chitosan electrospun mat directly placed onto the agar (Figure 35). This behavior was anticipated since the IR spectra (Figure 16) indicated the presence of positive active sites (NH_3^+), which are suggested to be responsible for interacting with negatively charged microbial cell membranes, which leads to leakage of intracellular components.[61,68,103]

It is possible that the presence of the remnant TFA solvent in the electrospun chitosan mats (as observed in the IR spectra, Figure 16), may have helped to increase the antimicrobial activity of chitosan. Torres-Giner et al.[61] reported reduction of *S. aureus* bacteria counts when controls with only TFA were used in the antimicrobial test. More importantly, no bacterial growth was observed when electrospun medium molecular weight chitosan was used.

The results obtained in the current study led us to partially reject the proposed null hypothesis that there would not be a significant difference in the effect of the physico-mechanical properties of the experimental sealants when compared to Helioseal Clear, a commercially available sealant; and to accept that there would not be a significant difference in the effect of the antibacterial properties of the experimental sealants when compared to Helioseal Clear. These conclusions were made since the overall results indicated that the chitosan groups presented significant higher flexural strength and hardness than any other group and no antibacterial effect was seen in any group tested in this study.

SUMMARY AND CONCLUSIONS

73

The purpose of this *in-vitro* study was to develop and evaluate an experimental resin-based sealant containing electrospun nylon-6 (N6) and chitosan (CH) nanofibers as an attempt to enhance the mechanical properties and provide an antibacterial protective effect, respectively. Electrospun nylon-6 and chitosan nanofibers mats were immersed into a resin mixture of monomers and polymerized to be submitted to a cryomilling process to obtain a fine micron-sized powder. Different filler levels were used to prepare the N6 and CH incorporated resin-based sealants (Table I). An unfilled experimental sealant and Helioseal Clear were used as controls. Three-point flexural testing, Vickers microhardness testing, and agar diffusion testing were used to test the experimental materials. The results indicated that overall, the chitosan groups presented significant higher flexural strength and hardness than the other groups. No bacteria inhibition was seen in any of the groups tested.

Further investigation is needed to evaluate whether the addition of a coupling agent, the increase of cryomilling time to reduce particle size, better particle dispersion, a different type of chitosan, and cross-linking of the chitosan nanofibers may enhance the physico-mechanical and antibacterial properties of the materials tested.

Within the limitations of this *in-vitro* study, the following conclusions were drawn:

1. Nylon-6 and chitosan mats were successfully prepared via electrospinning.

74

2. Nylon-6 did not enhance the physico-mechanical properties of the
   experimental resin-based sealants. Chitosan did not provide antibacterial
   properties to the experimental sealants.

REFERENCES

1.   Simonsen RJ. From prevention to therapy: minimal intervention with sealants and resin restorative materials. J Dent 2011;39 Suppl 2:S27-33.

2.   Simonsen RJ. Clinical applications of the acid etch technique. Chicago: Quintessence;1978.

3.   Wendt LK, Koch G. Fissure sealant in permanent first molars after 10 years. Swed Dent J 1988;12(5):181-5.

4.   Simonsen RJ. Retention and effectiveness of dental sealant after 15 years. J Am Dent Assoc 1991;122(10):34-42.

5.   Ahovuo-Saloranta A, Hiiri A, Nordblad A, Makela M, Worthington HV. Pit and fissure sealants for preventing dental decay in the permanent teeth of children and adolescents. Cochrane Database Syst Rev 2008(4):CD001830.

6.   Griffin SO, Oong E, Kohn W, et al. The effectiveness of sealants in managing caries lesions. J Dent Res 2008;87(2):169-74.

7.   Oong EM, Griffin SO, Kohn WG, Gooch BF, Caufield PW. The effect of dental sealants on bacteria levels in caries lesions: a review of the evidence. J Am Dent Assoc 2008;139(3):271-8; quiz 357-278.

8.   Martin J, Fernandez E, Estay J, Gordan VV, Mjor IA, Moncada G. Minimal invasive treatment for defective restorations: five-year results using sealants. Operative Dentistry 2013;38(2):125-33.

9.   Greiner A, Wendorff JH. Electrospinning: a fascinating method for the preparation of ultrathin fibers. Angewandte Chemie International Edition 2007;46(30):5670-703.

10.   Huang Z-M, Zhang Y-Z, Kotaki M, Ramakrishna S. A review on polymer nanofibers by electrospinning and their applications in nanocomposites. Composites Sci Technol 2003;63(15):2223-53.

11.   Schiffman JD, Schauer CL. Cross-linking chitosan nanofibers. Biomacromolecules 2007;8(2):594-601.

12.   Park BK, Kim MM. Applications of chitin and its derivatives in biological medicine. Int J Mol Sci 2010;11(12):5152-64.

13.   Maeda Y, Kimura Y. Antitumor effects of various low-molecular-weight chitosans are due to increased natural killer activity of intestinal intraepithelial lymphocytes in sarcoma 180-bearing mice. J Nutr Apr 2004;134(4):945-50.

14.   Ng KW, Khor HL, Hutmacher DW. In vitro characterization of natural and synthetic dermal matrices cultured with human dermal fibroblasts. Biomaterials 2004;25(14):2807-18.

15.   Synowiecki J, Al-Khateeb NA. Production, properties, and some new applications of chitin and its derivatives. Crit Rev Food Sci Nutr 2003;43(2):145-71.

16.   Walker-Simmons M, Hadwiger L, Ryan CA. Chitosans and pectic polysaccharides both induce the accumulation of the antifungal phytoalexin pisatin in pea pods and antinutrient proteinase inhibitors in tomato leaves. Biochem Biophys Res Commun 1983;110(1):194-9.

17.   Silva C, Cavaco-Paulo A. Biotransformations in synthetic fibres. Biocatalysis Biotransform 2008;26(5):350-6.

18.   Tajirian AL, Goldberg DJ. A review of sutures and other skin closure materials. J Cosmetic Laser Therapy 2010;12(6):296-302.

19.   Li Y, Swartz M, Phillips R, Moore B, Roberts T. Materials science effect of filler content and size on properties of composites. J Dent Res 1985;64(12):1396-1403.

20.   Dogan OM, Bolayir G, Keskin S, Dogan A, BEK B, Boztug A. The effect of esthetic fibers on impact resistance of a conventional heat-cured denture base resin. Dent Material J 2007;26(2):232-9.

21.   Uzun G, Hersek N, Tincer T. Effect of five woven fiber reinforcements on the impact and transverse strength of a denture base resin. J Prosthetic Dentistry 1999;81(5):616-20.

22.   Soto-Rojas AE, Escoffie-Ramirez M, Perez-Ferrera G, Guido JA, Mantilla-Rodriguez AA, Martinez-Mier EA. Retention of dental sealants placed on sound teeth and incipient caries lesions as part of a service-learning programme in rural areas in Mexico. Int J Paediatric Dentistry/ British Paedodontic Soc/ Int Assoc Dentistry Children 2012;22(6):451-8.

23.   Simonsen RJ. Glass ionomer as fissure sealant--a critical review. J Public Health Dentistry 1996;56(3 Spec No):146-9; discussion 161-143.

24.   Buonocore MG. A simple method of increasing the adhesion of acrylic filling materials to enamel surfaces. J Dent Res 1955;34(6):849-53.

25.   Cueto EI, Buonocore MG. Sealing of pits and fissures with an adhesive resin: its use in caries prevention. J Am Dent Assoc 1967;75(1):121-8.

26.   Gooch BF, Griffin SO, Gray SK, et al. Preventing dental caries through school-based sealant programs: updated recommendations and reviews of evidence. J Am Dent Assoc 2009;140(11):1356-65.

27.   Griffin SO, Oong E, Kohn W, et al. The effectiveness of sealants in managing caries lesions. J Dent Res 2008;87(2):169-74.

28.   Beauchamp J, Caufield PW, Crall JJ, et al. Evidence-based clinical recommendations for the use of pit-and-fissure sealants: a report of the American Dental Association Council on Scientific Affairs. J Am Dent Assoc 2008;139(3):257-68.

29.   Ripa LW. Sealants revisited: an update of the effectiveness of pit-and-fissure sealants. Caries Res 1993;27 Suppl 1:77-82.

30.   Kühnisch J, Mansmann U, Heinrich-Weltzien R, Hickel R. Longevity of materials for pit and fissure sealing. Results from a meta-analysis. Dent Material 2012;28(3):298-303.

31.   Kusgoz A, Tuzuner T, Ulker M, Kemer B, Saray O. Conversion degree, microhardness, microleakage and fluoride release of different fissure sealants. J Mechanic Behavior Biomed Material 2010;3(8):594-9.

32.   Jafarzadeh M, Malekafzali B, Tadayon N, Fallahi S. Retention of a flowable composite resin in comparison to a conventional resin-based sealant: one-year follow-up. J Dent (Tehran) 2010;7(1):1-5.

33.   Sakaguchi RL, Powers JM. Craig's restorative dental materials 2012; http://www.sciencedirect.com/science/book/9780323081085.

34.   Celiberti P, Lussi A. Penetration ability and microleakage of a fissure sealant applied on artificial and natural enamel fissure caries. J Dentistry 2007;35(1):59-67.

35.   Li Y, Swartz ML, Phillips RW, Moore BK, Roberts TA. Effect of filler content and size on properties of composites. J Dent Res 1985;64(12):1396-1401.

36.   Fong H. Electrospun nylon 6 nanofiber reinforced BIS-GMA/TEGDMA dental restorative composite resins. Polymer 2004;45(7):2427-32.

37.   Tian M, Gao Y, Liu Y, et al. Bis-GMA/TEGDMA dental composites reinforced with electrospun nylon 6 nanocomposite nanofibers containing highly aligned fibrillar silicate single crystals. Polymer (Guildf) 2007;48(9):2720-8.

38.   Korbmacher-Steiner HM, Schilling AF, Huck LG, Kahl-Nieke B, Amling M. Laboratory evaluation of toothbrush/toothpaste abrasion resistance after smooth enamel surface sealing. Clinical oral investigation 2013:1-10.

39.   Jensen ME, Wefel JS, Triolo PT, Hammesfahr PD. Effects of a fluoride-releasing fissure sealant on artificial enamel caries. Am J Dentistry 1990;3(2):75-8.

40.   Kantovitz KR, Pascon FM, Nociti FH, Jr., Tabchoury CP, Puppin-Rontani RM. Inhibition of enamel mineral loss by fissure sealant: an in situ study. J Dentistry 2013;41(1):42-50.

41.   Vatanatham K, Trairatvorakul C, Tantbirojn D. Effect of fluoride- and nonfluoride-containing resin sealants on mineral loss of incipient artificial carious lesion. J Clinical Pediatric Dentistry 2006;30(4):320-4.

42.   Naorungroj S, Wei HH, Arnold RR, Swift EJ, Jr., Walter R. Antibacterial surface properties of fluoride-containing resin-based sealants. J Dentistry 2010;38(5):387-91.

43.   Friedman M. Fluoride prolonged release preparations for topical use. J Dent Res 1980;59(8):1392-7.

44.   Cooley RL, McCourt JW. Evaluation of by SEM, microleakage, and fluoride release. Pediatric Dentistry 1990;12(1):39.

45.   Rock W, Foulkes E, Perry H, Smith A. A comparative study of fluoride-releasing composite resin and glass ionomer materials used as fissure sealants. J Dentistry 1996;24(4):275-80.

46.   Simonsen R, Neal R. A review of the clinical application and performance of pit and fissure sealants. Australian Dent J 2011;56(s1):45-58.

47.   Muller-Bolla M, Lupi-Pegurier L, Tardieu C, Velly AM, Antomarchi C. Retention of resin-based pit and fissure sealants: a systematic review. Community Dentistry Oral Epidemiol 2006;34(5):321-36.

48.   Silva KG, Pedrini D, Delbem AC, Ferreira L, Cannon M. In situ evaluation of the remineralizing capacity of pit and fissure sealants containing amorphous calcium phosphate and/or fluoride. Acta Odontologica Scandinavica 2010;68(1):11-8.

49.   Li F, Li F, Wu D, et al. The effect of an antibacterial monomer on the antibacterial activity and mechanical properties of a pit-and-fissure sealant. J Am Dent Assoc 2011;142(2):184-93.

50.   Shimazu K, Ogata K, Karibe H. Evaluation of the ion-releasing and recharging abilities of a resin-based fissure sealant containing S-PRG filler. Dent Material J 2011(0):11112-20211.

51.   Greiner A, Wendorff JH. Electrospinning: a fascinating method for the preparation of ultrathin fibers. Angew Chem Int Ed Engl 2007;46(30):5670-703.

52.   Chronakis IS. Novel nanocomposites and nanoceramics based on polymer nanofibers using electrospinning process -- a review. J Material Processing Technol 2005;167(2-3):283-93.

53.   Jean-Gilles R, Soscia D, Sequeira S, et al. Novel modeling approach to generate a polymeric nanofiber scaffold for salivary gland cells. J Nanotechnol Eng Med 2010;1(3):31008.

54.   Lu X, Wang C, Wei Y. One-dimensional composite nanomaterials: synthesis by electrospinning and their applications. Small 2009;5(21):2349-70.

55.   Kumar MN. A review of chitin and chitosan applications. React Funct Polym 2000;46:1-27.

56.   Park BK, Kim M-M. Applications of chitin and its derivatives in biological medicine. Int J Molecular Sci 2010;11(12):5152-64.

57.   Matsunaga T, Yanagiguchi K, Yamada S, Ohara N, Ikeda T, Hayashi Y. Chitosan monomer promotes tissue regeneration on dental pulp wounds. J Biomedical Material Res Part A 2006;76(4):711-20.

58.   Muzzarelli R, Biagini G, Bellardini M, Simonelli L, Castaldini C, Fratto G. Osteoconduction exerted by methylpyrrolidinone chitosan used in dental surgery. Biomaterials 1993;14(1):39-43.

59.   Arancibia R, Maturana C, Silva D, et al. Effects of chitosan particles in periodontal pathogens and gingival fibroblasts. J Dental Res 2013.

60.   Mahapoka E, Arirachakaran P, Watthanaphanit A, Rujiravanit R, Poolthong S. Chitosan whiskers from shrimp shells incorporated into dimethacrylate-based dental resin sealant. Dent Material J 2012;31(2):273-9.

61.   Torres-Giner S, Ocio M, Lagaron J. Development of active antimicrobial fiber-based chitosan polysaccharide nanostructures using electrospinning. Eng Life Sci 2008;8(3):303-14.

62.   Mellegard H, Strand SP, Christensen BE, Granum PE, Hardy SP. Antibacterial activity of chemically defined chitosans: influence of molecular weight, degree of acetylation and test organism. Int J Food Microbiol 2011;148(1):48-54.

63.   Seyfarth F, Schliemann S, Elsner P, Hipler UC. Antifungal effect of high- and low-molecular-weight chitosan hydrochloride, carboxymethyl chitosan, chitosan

oligosaccharide and N-acetyl-D-glucosamine against Candida albicans, Candida krusei and Candida glabrata. Int J Pharm 2008;353(1-2):139-48.

64.   Rabea EI, Badawy ME, Stevens CV, Smagghe G, Steurbaut W. Chitosan as antimicrobial agent: applications and mode of action. Biomacromolecules 2003;4(6):1457-65.

65.   Liu H, Du Y, Wang X, Sun L. Chitosan kills bacteria through cell membrane damage. Int J Food Microbiol 2004;95(2):147-55.

66.   Kong M, Chen XG, Xing K, Park HJ. Antimicrobial properties of chitosan and mode of action: a state of the art review. Int J Food Microbiol 2010;144(1):51-63.

67.   Sudarshan NR, Hoover DG, Knorr D. Antibacterial action of chitosan. Food Biotechnol 1992;6(3):257-72.

68.   Aider M. Chitosan application for active bio-based films production and potential in the food industry: review. LWT-Food Sci Technol 2010;43(6):837-42.

69.   Balakrishnan M, Simmonds RS, Tagg JR. Dental caries is a preventable infectious disease. Aust Dent J 2000;45(4):235-45.

70.   Huang R, Li M, Gregory RL. Bacterial interactions in dental biofilm. Virulence. 2011;2(5):435-44.

71.   Tarsi R, Muzzarelli RA, Guzman CA, Pruzzo C. Inhibition of Streptococcus mutans adsorption to hydroxyapatite by low-molecular-weight chitosans. J Dent Res 1997;76(2):665-72.

72.   Chavez de Paz LE, Resin A, Howard KA, Sutherland DS, Wejse PL. Antimicrobial effect of chitosan nanoparticles on streptococcus mutans biofilms. Appl Environ Microbiol 2011;77(11):3892-5.

73.   Neilands J, Sutherland D, Resin A, Wejse PL, Chavez de Paz LE. Chitosan nanoparticles affect the acid tolerance response in adhered cells of Streptococcus mutans. Caries Res 2011;45(6):501-5.

74.   Levchik SV, Weil ED, Lewin M. Thermal decomposition of aliphatic nylons. Polymer Int 1999;48(7):532-57.

75.   Hang F, Lu D, Bailey RJ, et al. In situ tensile testing of nanofibers by combining atomic force microscopy and scanning electron microscopy. Nanotechnol 2011;22(36):365708.

76.   Stachewicz U, Peker I, Tu W, Barber AH. Stress delocalization in crack tolerant electrospun nanofiber networks. ACS Appl Mater Interfaces 2011;3(6):1991-6.

77.   Reneker DH, Yarin AL, Fong H, Koombhongse S. Bending instability of electrically charged liquid jets of polymer solutions in electrospinning. J Applied Physics 2000;87:4531.

78.   Tian M, Gao Y, Liu Y, et al. Bis-GMA/TEGDMA dental composites reinforced with electrospun nylon 6 nanocomposite nanofibers containing highly aligned fibrillar silicate single crystals. Polymer 2007;48(9):2720-8.

79.   Jiang S, Hou H, Greiner A, Agarwal S. Tough and transparent nylon-6 electrospun nanofiber reinforced melamine-formaldehyde composites. ACS Appl Mater Interfaces 2012;4(5):2597-2603.

80.   Chen L-S, Huang Z-M, Dong G-H, et al. Development of a transparent PMMA composite reinforced with nanofibers. Polymer Composites 2009;30(3):239-47.

81.   Romo-Uribe A, Arizmendi L, Romero-Guzman ME, Sepulveda-Guzman S, Cruz-Silva R. Electrospun nylon nanofibers as effective reinforcement to polyaniline membranes. ACS Appl Mater Interfaces 2009;1(11):2502-8.

82.   Sencadas V, Correia D, Areias A, et al. Determination of the parameters affecting electrospun chitosan fiber size distribution and morphology. Carbohydrate Polymers 2012;87(2):1295-1301.

83.   Osorio E, Osorio R, Davidenko N, Sastre R, Aguilar JA, Toledano M. Polymerization kinetics and mechanical characterization of new formulations of light-cured dental sealants. J Biomed Mater Res B Appl Biomater 2007;80(1):18-24.

84.   Sun W, Cai Q, Li P, et al. Post-draw PAN-PMMA nanofiber reinforced and toughened Bis-GMA dental restorative composite. Dent Mater 2010;26(9):873-80.

85.   Lee K-H, Kim K-W, Pesapane A, Kim H-Y, Rabolt JF. Polarized FT-IR study of macroscopically oriented electrospun nylon-6 nanofibers. Macromolecules 2008;41(4):1494-8.

86.   Sangsanoh P, Supaphol P. Stability improvement of electrospun chitosan nanofibrous membranes in neutral or weak basic aqueous solutions. Biomacromolecules 2006;7(10):2710-14.

87.   Amaral I, Granja P, Barbosa M. Chemical modification of chitosan by phosphorylation: an XPS, FT-IR and SEM study. J Biomaterial Sci, Polymer Edition 2005;16(12):1575-93.

88.   Zhao Y, Yang Q, Lu X-F, Wang C, Wei Y. Study on correlation of morphology of electrospun products of polyacrylamide with ultrahigh molecular weight. J Polymer Sci Part B: Polymer Physics 2005;43(16):2190-5.

89.   Qian D, Dickey EC, Andrews R, Rantell T. Load transfer and deformation mechanisms in carbon nanotube-polystyrene composites. Applied Physics Letters 2000;76:2868.

90.   Zhang X, Zhang X, Zhu B, Lin K, Chang J. Mechanical and thermal properties of denture PMMA reinforced with silanized aluminum borate whiskers. Dent Material J 2012;31(6):903-8.

91.   Nihei T, Dabanoglu A, Teranaka T, et al. Three-body-wear resistance of the experimental composites containing filler treated with hydrophobic silane coupling agents. Dent Material 2008;24(6):760-4.

92.   Fu S-Y, Feng X-Q, Lauke B, Mai Y-W. Effects of particle size, particle/matrix interface adhesion and particle loading on mechanical properties of particulate–polymer composites. Composites Part B: Eng 2008;39(6):933-61.

93.   McDonough WG, Antonucci JM, Dunkers JP. Interfacial shear strengths of dental resin-glass fibers by the microbond test. Dent Material 2001;17(6):492-8.

94.   Ou Y, Yang F, Yu ZZ. A new conception on the toughness of nylon 6/silica nanocomposite prepared via in situ polymerization. J Polymer Sci Part B: Polymer Physics 1998;36(5):789-95.

95.   Jiang L, Wang F, Han F, Prinyawiwatkul W, No HK, Ge B. Evaluation of diffusion and dilution methods to determine the antimicrobial activity of water-soluble chitosan derivatives. J Applied Microbiol 2013.

96.   Gaudreau C, Girouard Y, Ringuette L, Tsimiklis C. Comparison of disk diffusion and agar dilution methods for erythromycin and ciprofloxacin susceptibility testing of Campylobacter jejuni subsp. jejuni. Antimicrobial Agents Chemotherapy 2007;51(4):1524-6.

97.   Goy RC, de Britto D, Assis OB. A review of the antimicrobial activity of chitosan. Polímeros:Ciência e Tecnologia 2009;19(3):241-7.

98.   Lebrun L, Junter G-A. Diffusion of sucrose and dextran through agar gel membranes. Enzyme Microbial Technol 1993;15(12):1057-62

99.   Rodríguez-Núñez JR, López-Cervantes J, Sánchez-Machado DI, Ramírez-Wong B, Torres-Chavez P, Cortez-Rocha MO. Antimicrobial activity of chitosan-based films against Salmonella typhimurium and Staphylococcus aureus. Int J Food Sci Technol 2012;47(10):2127-33.

100.   Muzzarelli R, Tarsi R, Filippini O, Giovanetti E, Biagini G, Varaldo P. Antimicrobial properties of N-carboxybutyl chitosan. Antimicrobial agents and chemotherapy 1990;34(10):2019-23.

101.   Hosseini MH, Razavi SH, Mousavi SMA, Yasaghi SAS, Hasansaraei AG. Improving antibacterial activity of edible films based on chitosan by incorporating thyme and clove essential oils and EDTA. J Applied Sci 2008;8(16):2895-900.

102.   Tripathi S, Mehrotra G, Dutta P. Chitosan–silver oxide nanocomposite film: Preparation and antimicrobial activity. Bull Materials Sci 2011;34(1):29-35.

103.   Helander I, Nurmiaho-Lassila E-L, Ahvenainen R, Rhoades J, Roller S. Chitosan disrupts the barrier properties of the outer membrane of Gram-negative bacteria. Int J Food Microbiol 2001;71(2):235-44.

ABSTRACT

EFFECT OF NYLON-6 AND CHITOSAN NANOFIBERS ON THE PHYSICO-MECHANICAL AND ANTIBACTERIAL PROPERTIES OF AN EXPERIMENTAL RESIN-BASED SEALANT

by

Maria Fernanda Hamilton

Indiana University School of Dentistry
Indianapolis, Indiana

Purpose: Dental sealant forms a physical barrier to prevent pit and fissure caries; therefore, the retention rate becomes a main factor of the sealant's effectiveness. Electrospun nylon-6/N6 nanofibers have shown good mechanical properties, such as high tensile strength and fracture toughness. Chitosan/CH has received significant attention due to properties such as antibacterial activity. The purpose of this study was to synthesize and evaluate the effect of incorporating N6 and CH electrospun nanofibers on the physical-mechanical and antibacterial properties of an experimental resin-based sealant. Methods and Materials: Nanofiber synthesis: N6 pellets were dissolved in 1,1,1,3,3,3-hexafluoro-2-propanol at a concentration of 10wt%. Practical-grade chitosan was dissolved in trifluoroacetic acid and dichloromethane (60:40 TFA/DCM) at 7 wt%.

Electrospinning parameters were optimized in order to fabricate defect-free N6 and chitosan nanofiber mats. Morphological and chemical characterizations were performed by scanning electron microscopy (SEM) and Fourier transform infrared (FTIR) spectroscopy, respectively after vacuum drying the mats for 48 h. The average fiber diameter was determined from SEM images by measuring the diameter of 120 fibers using ImageJ software. Experimental Sealant: N6 and CH electrospun mats (3×3cm^2) were immersed into a resin mixture of BIS-GMA/TEGDMA. Once no bubbles were seen, the resin-modified N6 and CH mats were put on a glass plate, light-cured ("TRIAD 2000") for 2 min and then submitted to a cryomilling process to obtain a fine micron-sized powder. Three different filler levels (1 wt%, 2.5 wt%, 5 wt%) were used to prepare the N6 and CH incorporated resin-based sealants. Additionally, a commercially available resin-based sealant and the experimental resin mixture (unfilled) were used as controls. Three-point flexural testing, Vickers microhardness testing, and agar diffusion testing were performed on the experimental sealants and the commercial sealant. Data were analyzed by one-way ANOVA and Fisher's Protected Least Significant Differences Pair-wise comparisons between groups (5%). Results: The average fiber diameter for N6 was found to be 503±304 nm and 595±411 nm for CH. No significant difference was found between fiber diameter ($p = 0.0601$). FTIR confirmed the characteristic peaks for N6 ((CO-NH and [-(CH$_2$)$_5$-].) and CH (N-H and C$_2$F$_3$O$_2^-$). CH-5% group had significantly higher ($p = 0.0000$) FS (115.3±4.5 MPa) than all other groups. CH-1% and CH-2.5% groups had significantly higher FS than the control (unfilled) ($p = 0.0016$ and $p = 0.0033$ respectively); Helioseal Clear ($p = 0.0000$), and nylon groups. N6-5% had significantly higher flexural strength than Helioseal Clear ($p = 0.0013$) and N6-2.5% ($p = 0.0250$).

CH-1% had significantly higher hardness values than all other groups, and CH-5% (p = 0.0414) had significantly higher values than N6-2.5%. No antibacterial inhibition was seen in any of the tested groups. Conclusions: CH and N6 nanofibers were successfully prepared via electrospinning and used to modify the experimental resin-based dental sealants. The overall results indicated that CH-containing sealants presented the highest flexural strength and hardness; however, none of the CH groups displayed antimicrobial properties. Further investigation is needed to enhance the physico-mechanical properties of the experimental resin-based sealants using nylon-6 and CH.

CURRICULUM VITAE

Maria Fernanda Hamilton

May 1981	Born in Cuenca, Ecuador
September 2005	Doctor of Dental Surgery (D.D.S) Universidad de Cuenca, Dental School Cuenca, Ecuador
September to October 2005	General Practice Ministerio de Salud Publica Area de Salud No. 9 Nabon, Ecuador
October 2005 to October 2006	Specialization Degree on Endodontics Faculdade Inga, Uninga. Post-Graduation Unit Bauru Sao Paulo - Brazil
December 2006 to January 2007	Endodontist Private Practice Cuenca, Ecuador
July 2011 to May 2013	Bench Instructor for Pre-Doctoral Dental Students Indiana University School of Dentistry Indianapolis, Indiana
2010 to May 2014	Master of Science in Dentistry, Operative and Preventive Dentistry Indiana University School of Dentistry Indianapolis, Indiana

Professional Organizations

Awards American Dental Education Association
Indiana Section of the American Association for Dental Research

Awards

January 2012 to May 2012	Sam H. Jones Community Service Scholarship
August 2012 to May 2013	Sam H. Jones Community Service Scholarship